

Received November 19, 2019, accepted December 2, 2019, date of publication December 5, 2019, date of current version December 23, 2019.

Digital Object Identifier 10.1109/ACCESS.2019.2957763

Dual-Beam and Tri-Band SIW Leaky-Wave Antenna With Wide Beam Scanning Range Including Broadside Direction

YUNJIE GENG^{ID}, JUNHONG WANG^{ID}, (Senior Member, IEEE), ZHENG LI^{ID}, (Member, IEEE), YUJIAN LI^{ID}, (Member, IEEE), MEIE CHEN^{ID}, AND ZHAN ZHANG^{ID}

Key Laboratory of All Optical Network and Advanced Telecommunication Network of MOE, Beijing Jiaotong University, Beijing 100044, China
Institute of Lightwave Technology, Beijing Jiaotong University, Beijing 100044, China

Corresponding author: Junhong Wang (wangjunh@bjtu.edu.cn)

This work was supported by the National Nature Science Foundation of China (NSFC) Project under Grant 61871025.

ABSTRACT In this letter, a novel dual-beam and tri-band leaky-wave antenna (LWA) based on substrate integrated waveguide (SIW) structure is proposed, which has the capability of wide beam scanning range including broadside direction. The antenna consists of two kinds of periodic structures which can excite two -1st spatial harmonic waves and result in two radiation beams simultaneously. Through theoretical dispersion diagram analysis of the unit cells of two periodic structures and by applying the techniques of impedance-matching and reflection-cancelling, the open-stopbands at broadside are suppressed. Then the main beam of the proposed LWA can scan from backward to forward through broadside when frequency changes. Moreover, a tri-band application can be achieved in the dual-beam antenna by optimization of the second periodic structure. The measured results validate that the proposed SIW LWA has three operating frequency bands. In band 1 from 8.6 to 9.2 GHz, there is one beam scanning from 42° to 71° in the forward, in band 2 from 10 to 12 GHz, there is one beam scanning from -40° to 4° in the backward, and in band 3 from 12.5 to 15 GHz, there is a dual-beam scanning from -55° to 54° including broadside direction, which show good agreements with the simulated results.

INDEX TERMS Dual-beam, tri-band, open-stopband (OSB), leaky-wave antenna (LWA), substrate integrated waveguide (SIW).

I. INTRODUCTION

Leaky-wave antennas (LWAs) have attracted significant attentions in microwave and millimeter-wave regions due to their simple feeding network, frequency beam scanning capability and high directivity [1]. These features make leaky-wave antenna a good candidate for modern wireless communication systems, e.g. automotive radar sensor [2], analog real-time spectrum analyzer [3], and the fifth generation (5G) mobile communication [4].

Generally, LWAs are classified as uniform structures [5], [6] and periodic structures [7], [8] based on the guiding wave systems. A typical uniform LWA is usually designed based on wave-guiding structure supporting fast-wave on fundamental ($n = 0$) mode, whose beam can only scan in

forward region. The periodic LWA is formed by introducing periodic unit cells along slow-wave guiding structure. The slow-wave structure itself is a non-radiation structure, but the introduced periodic unit cells can excite infinite spatial harmonics, some of which are locating in the fast-wave region, such as the -1st spatial harmonic ($n = -1$) mode, and can leak away from the structure. The periodic LWAs can steer their main beams not only in the forward directions but also in the backward directions, except for a narrow angular region near the broadside direction, where an open-stopband (OSB) occurs [1]. In the open-stopband region, a large reflection coefficient is encountered and the radiation power drops substantially.

For the OSB suppression of periodic LWAs, several techniques are proposed, such as impedance-matching [9]–[12], reflection-cancelling [13], [14], and using asymmetric structure [15], [16], etc. In [11], a simple technique is presented

The associate editor coordinating the review of this manuscript and approving it for publication was Kai Lu^{ID}.

for suppression of OSB in periodic LWAs using two similar but non-identical elements. With this technique, one only needs to optimize the distance between the two elements and the dimension of the second element. In [12], a substrate integrated waveguide (SIW) leaky-wave antenna with wide angular beam scanning is presented, in which a longitudinal slot and an inductive post are placed oppositely and offset from the center line. By introducing the inductive post along with the longitudinal slot, the OSB of the proposed antenna is suppressed, and a continuous beam scanning including broadside is achieved.

In modern wireless communication and detection systems, such as personal and vehicular communications, collision avoidance system, radar sensor and radar-tracking systems, dual-beam or multi-beam antennas are usually desired [17]. These antennas can transmit and receive signals to and from different directions simultaneously, which exhibit flexibility in communication with more objects simultaneously. In order to excite two radiation beams, various methods are applied in the design of LWAs. In [18] and [19], the dual-beam radiation is realized by using two feeding ports and center-feeding structure, respectively. In [20] and [21], the second higher order mode of micro-CPW LWA and both TE₁₀ and TE₀₁ modes of a SIW LWA are used to generate the dual-beam radiation, respectively. In [22] and [23], two dual-beam LWAs using active components are demonstrated. In [24] and [25], two multiple periodic structures are presented for asymmetric beam-scanning.

Multi-band leaky-wave antenna can work in several bands and reduce the volume of wireless communication system [26]. Many efforts focused on the realization of multi-band LWAs have been made, in which different transmission lines are used, such as generalized negative-refractive-index (NRI) transmission-line [27], mu-negative (MNG) transmission line [28], composite right-/left-hand (CRLH) transmission line [29], [30], and the U-slot [31] and L-slot [32] half-width microstrip line (MSL). Most of them are constructed by utilizing periodic unit cells with nonlinear dispersion characteristics. Recently, several dual-band LWAs based on the slotted SIW structures are proposed. In [33], an antenna consisting of two back-to-back slotted SIW arrays fed by two strip lines in a simple way is proposed, which can realize frequency-controlled beam scanning in two bands. In [34], a dual-band and dual-polarized SIW leaky-wave antenna with periodic transverse slots etched on the top plane and periodic circular slots on the bottom plane is investigated.

In this paper, a novel dual-beam and tri-band SIW LWA with beam scanning in a wide angular range including broadside direction is presented. Two kinds of periodic structures are used to support the dual-beam radiation, and impedance-matching and reflection-cancelling techniques are used to suppress the OSB. Moreover, the second periodic structure is optimized by introducing multiple periodic slots for the tri-band application. The design of dual-beam radiation and optimization of three frequency bands of the

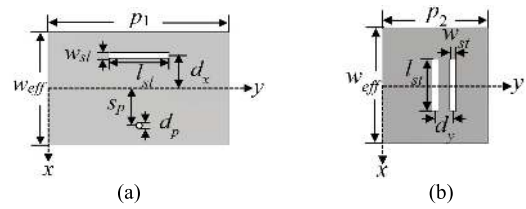


FIGURE 1. Unit cells of (a) the first periodic structure and (b) the second periodic structure.

proposed antenna are given in Section II. The measurement results and discussion are shown in Section III. The conclusions are drawn in Section IV.

II. DESIGN AND OPTIMIZATION

A. DESIGN OF DUAL-BEAM RADIATION

Fig. 1 gives the unit cells of the two periodic waveguide structures with different periods p_1 and p_2 , the width w_{eff} and thickness h of the two structures are the same, and the permittivity of substrate is $\epsilon_r = 3.66$, which is chosen among the available dielectric material considering the trade-off between operating frequency, size and efficiency of the antenna [11]. The first unit cell, as shown in Fig. 1 (a), consists of a longitudinal (y-direction) slot with length l_{sl} and width w_{sl} , and an inductive post with diameter d_p . The longitudinal slot is located in one side of the waveguide with an offset distance d_x from the center line of waveguide, and the post is placed in the other side of slot with an offset distance s_p from the center line of waveguide. The longitudinal slot and metallic post provide capacitive and inductive effect, respectively. By adjusting the diameter of post and the offset distance from the center line, the impedance-matching is achieved, and the OSB can be suppressed [12]. The second unit cell, as given in Fig. 1 (b), contains two transverse (x-direction) slots with identical length l_{st} and width w_{st} . The distance d_y between them is approximately a quarter of the period p_2 , which is optimized to cancel the reflection and mitigate the OSB [11]. All the parameters mentioned in Fig. 1 are listed in Table 1.

Fig. 2 gives the simulated dispersion diagram of the two unit cells, in which the suppression of OSB can be explained by the properties of phase constant β and attenuation constant α , calculated by [10]

$$|\beta| = \frac{1}{p} \operatorname{Re} \left[\cos^{-1} \left(\frac{1 - S_{11}S_{22} + S_{12}S_{21}}{2S_{21}} \right) \right] \quad (1-1)$$

$$|\alpha| = \frac{1}{p} \operatorname{Im} \left[\cos^{-1} \left(\frac{1 - S_{11}S_{22} + S_{12}S_{21}}{2S_{21}} \right) \right] \quad (1-2)$$

As pointed out in [11], the suppression of the open stop-band can be performed by a linear curve of the normalized phase constant and a flat curve of the normalized attenuation constant against the frequency around broadside. In Fig. 2, the phase delay $|\beta \cdot p|$ and attenuation $|\alpha \cdot p|$ of the two unit cells are depicted together and compared with $k_0 \cdot p$. The decreasing and increasing parts of $|\beta \cdot p|$ curve are corresponding to the backward and forward radiation, respectively.

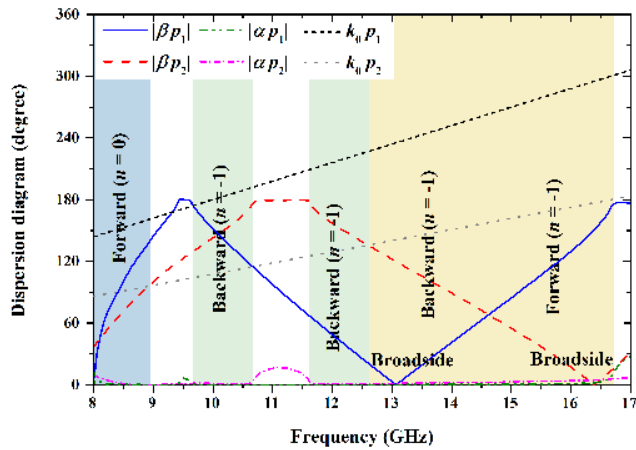


FIGURE 2. Simulated dispersion diagram of the unit cells of the two periodic structures.

One can observe that in the yellow part (nearly from 12.5 to 16.5 GHz), there are two -1st spatial harmonic waves which can radiate ($|\beta \cdot p_1| < k_0 \cdot p_1$ and $|\beta \cdot p_2| < k_0 \cdot p_2$). The first periodic structure can generate a beam scanning from broadside (around 13 GHz) to forward, as denoted by the blue line. The second periodic structure can generate a beam scanning from backward to broadside (near 16.5 GHz), as denoted by the red dotted line. As we can see, the attenuation curves ($|\alpha \cdot p_1|$ and $|\alpha \cdot p_2|$) of the two unit cells are flat around broadside direction, which indicate that the OSBs are suppressed for both two periodic structures.

Fig. 3 shows the whole configurations of two SIW LWAs constructed by cascading the unit cells in Fig. 1. The length and width of antennas are L and W . It's worth noting that, the adjacent unit cells of first LWA are placed asymmetrically, the slots and posts in adjacent cells are arranged oppositely, so the period of unit cell is reduced by half (i.e., $p_1 = 7.5$ mm). This arrangement allows more longitudinal slots to exist in a fixed-length waveguide, which will enhance the radiation efficiency and reduce the cross-polarization compared with the side by side design [12]. The transvers slots of second LWA at two ends of waveguide are tapered to realize a better impedance matching. The detail view of the microstrip feeding line with length l_m and width w_m , and the tapered section with length l_t and width w_t is shown in Fig. 3 (c). The SIW structure with width a , diameter of vias d and adjacent vias distance s is also given. The values of all parameters shown in Fig. 3 (c) are summarized in Table 1.

Fig. 4 shows the simulated S -parameters of two LWAs. One can observe that for two LWAs, the open-stopbands around broadside are suppressed and the $|S_{11}|$ is lower than -10 dB in the whole passband, except the stopband (from 10.7 to 11.7 GHz) between the fundamental mode and the -1st spatial harmonic mode of the second LWA. The reason for the elimination of corresponding stopband (from 9.3 to 9.6 GHz) in the first LWA is due to the asymmetric arrangement of the unit cells. The simulated gain patterns in yo -plane of two LWAs at different frequencies are shown in Fig. 5. Continuous beam

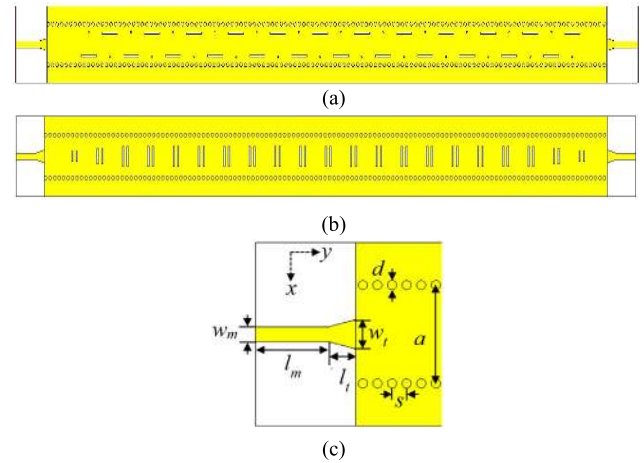


FIGURE 3. Configurations of two SIW LWAs: (a) complete view of the first LWA, (b) complete view of the second LWA, (c) detail view of the microstrip line and structure of SIW.

TABLE 1. Detail values of all parameters in this work (unit: mm).

Parameter	Value	Parameter	Value	Parameter	Value
p_1	15	d_x	3	s	1.6
p_2	9	d_y	1.6	d	1
l_{sl}	5.5	d'_y	1.5	l_m	8
w_{sl}	0.5	d_p	0.5	w_m	1.6
l_{st}	5	s_p	3.2	l_t	3
l'_{st}	4	h	1.524	w_t	3.2
l''_{st}	3	w_{eff}	10	L	222
w_{st}	0.5	a	10.7	W	20

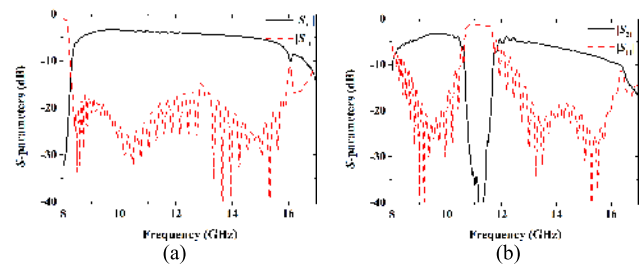


FIGURE 4. Simulated S -parameters of the two LWAs: (a) first LWA, (b) second LWA.

scanning from backward to forward including broadside can be observed in Fig. 5 (a) for the first LWA. In Fig. 5 (b), the main beam of the second LWA scans only from backward to broadside due to occurrence of the second higher mode of waveguide TE_{20} when frequency exceeds two times of the cut-off frequency.

Fig. 6 (a) demonstrates the configuration of proposed dual-beam SIW LWA based on the combinations of two periodic structures as shown in Fig. 3. As we can see, two kinds of periodic structures (the longitudinal slots with posts and pairs of transvers slots) can be etched on the top wall of waveguide simultaneously by proper design of structure parameters. The simulated S -parameters and gain patterns of the dual-beam

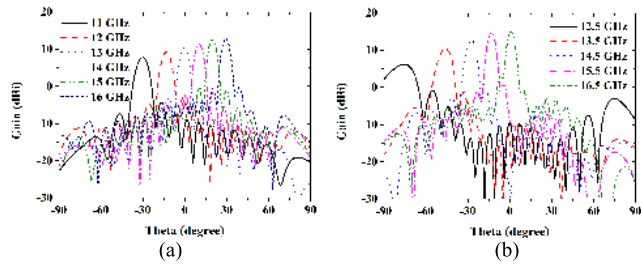


FIGURE 5. Simulated gain patterns (yoz-plane) of two LWAs at different frequencies: (a) first LWA, (b) second LWA.

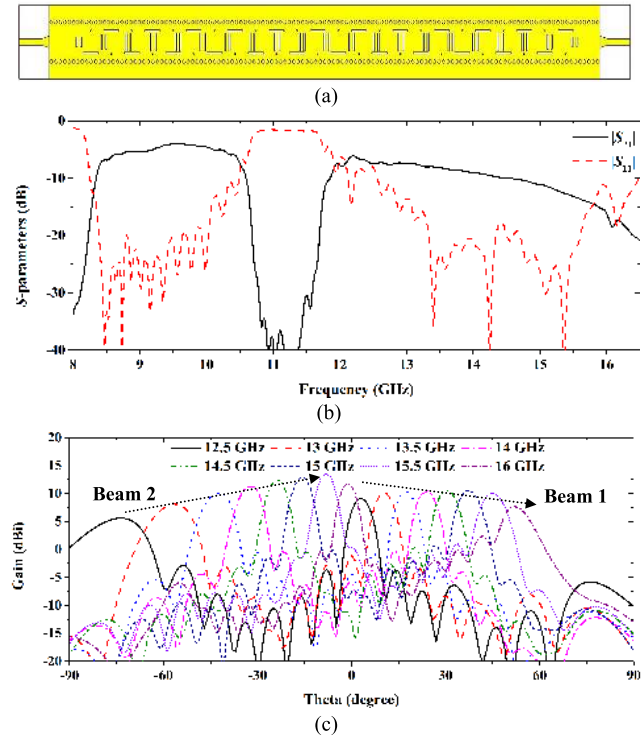


FIGURE 6. Simulated results of the proposed antenna with dual-beam radiation: (a) configurations, (b) S -parameters, (c) gain patterns (yoz-plane) at different frequencies.

antenna are plotted in Fig. 6 (b) and (c) respectively. Because the first LWA is a high-pass structure in the total band from 8.5 to 16.5 GHz as can be seen from Fig. 4 (a), the S -parameters of the dual-beam antenna is similar to that of the second LWA as shown in Fig. 4 (b), except for the transmission coefficient $|S_{21}|$ is lower due to increasing of radiation slots. Fig. 6 (c) shows that there are two beams radiating from the proposed antenna. Beam 1 is generated by the first periodic structure, scanning from 3° to 52° and beam 2 is generated by the second periodic structure, scanning from -74° to -1° when frequency changes from 12.5 GHz to 16 GHz.

B. OPTIMIZATION FOR TRI-BAND APPLICATION

We can see from the dispersion diagrams of two unit cells plotted in Fig. 2, there are another two bands in the low

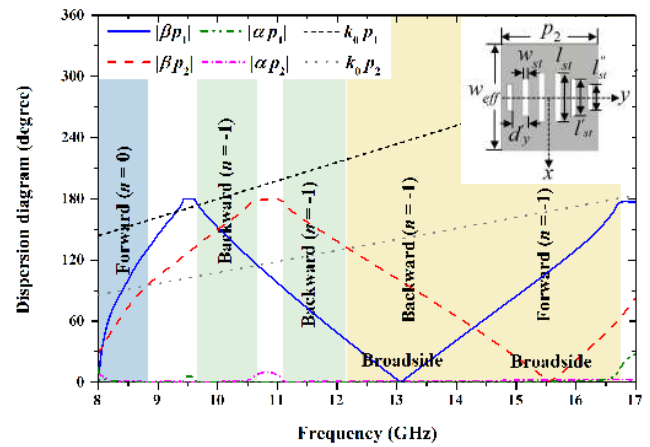


FIGURE 7. Unit cell and dispersion diagram of the optimized second periodic structure.

frequency with single-beam radiation. In band 2 (green part, nearly from 10 to 12.5 GHz except the stopband of second periodic structure from 10.7 to 11.7 GHz), the -1st spatial harmonic wave of first periodic structure will leak away ($|\beta \cdot p_1| < k_0 \cdot p_1$) and radiate in backward directions. In band 1 (blue part, nearly from 8 to 9 GHz), the fundamental waves ($n = 0$) of these two periodic structures both can radiate theoretically. However, because the parameters of two unit cells are designed to make the antenna work on the -1st spatial harmonic mode in band 3 to generate the dual-beam radiation, the radiation of fundamental wave in band 1 is not obvious. In this section, in consideration of the difficulty of design and implementation, we will optimize the unit cell of second LWA to realize the tri-band application for the proposed dual-beam antenna.

Fig. 7 gives the unit cell and dispersion diagram of the optimized second LWA. Compared with the unit cell of original second LWA as shown in Fig. 1 (b), only the slots etched on the top wall of waveguide are changed, i.e., the two identical transverse slots are extended to six symmetric (about x -axis) transverse slots with identical width w_{st} but different lengths l_{st} , l'_{st} and l''_{st} . The distance between two adjacent slots d'_y are adjusted according to the simulated dispersion diagram to suppress the OSB. Compared with the dispersion diagram of original design shown in Fig. 2, the frequency of broadside radiation for the optimized second structure is reduced from 16.5 GHz to 15.5 GHz and the stopband between the fundamental wave and the -1st spatial harmonic wave becomes smaller too, which means the scanning rate of this optimized structure has been enhanced due to the introduction of multiple periodic slots [35].

Fig. 8 shows the whole configuration of the optimized second LWA and its simulated S -parameters. The simulated radiation patterns of it at different frequencies in two bands (band 1 and band 3) are given in Fig. 9. As we can see from the simulated results, the optimized second LWA works on the fundamental mode in the low band (band 1) with forward scanning beam and works on the -1st spatial harmonic mode

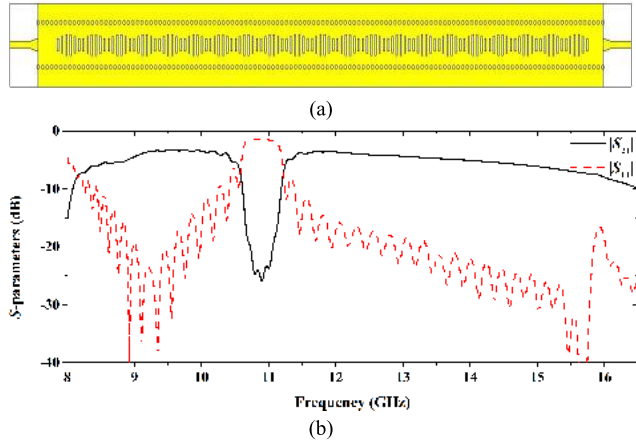


FIGURE 8. Simulated results of the optimized second LWA: (a) configuration, (b) S-parameters.

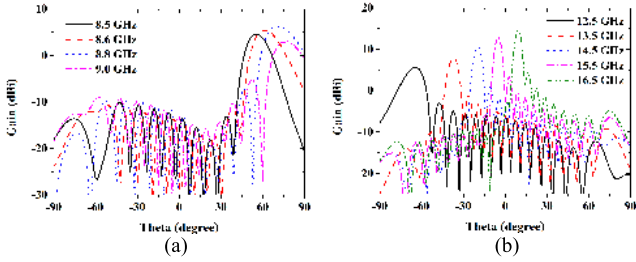


FIGURE 9. Simulated radiation patterns (yoz-plane) of the optimized second LWA at different frequencies: (a) band 1, (b) band 3.

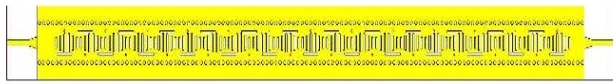


FIGURE 10. Configuration of the optimized antenna for tri-band applications.

in the high band (band 3) with the beam-scanning capability from backward to forward including broadside.

The whole configuration of the optimized dual-beam antenna for tri-band application is illustrated in Fig. 10. Fig. 11 (a)–(c) plot the simulated gain patterns of the proposed antenna at different frequencies in three bands, from which we can see, there is one beam scanning from 44° to 74° in forward region within the band from 8.6 to 9.2 GHz, one beam scanning from -41° to 2° in backward region within the band from 10 to 12 GHz, and two beams scanning from -61° to 57° including broadside direction within the band from 12.5 to 15.5 GHz. The cross-pol level of this antenna in the three bands are around -20 dB as can be observed from Fig. 11.

III. MEASUREMENT AND DISCUSSION

Fig. 12 (a) shows the fabricated prototype of the proposed dual-beam and tri-band SIW LWA with the SMA connectors. The prototype is fabricated using Rogers RO4350B substrate with thickness of $h = 1.524$ mm and dielectric constant

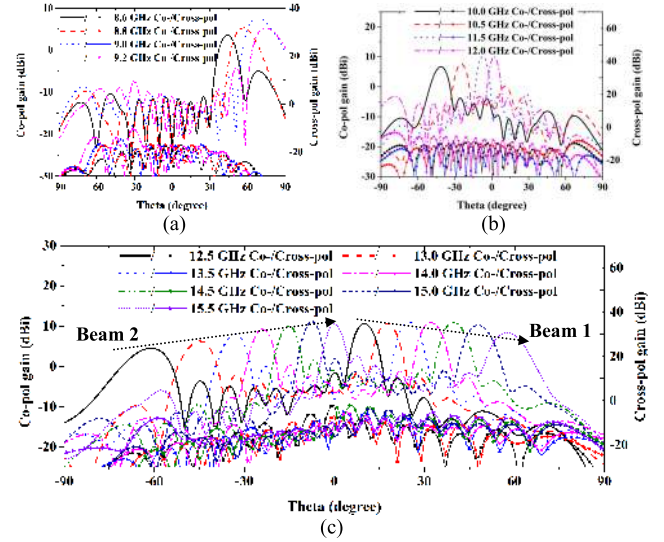


FIGURE 11. Simulated gain patterns (yoz-plane) of the optimized antennas in different frequency bands: (a) band 1, (b) band 2, (c) band 3.

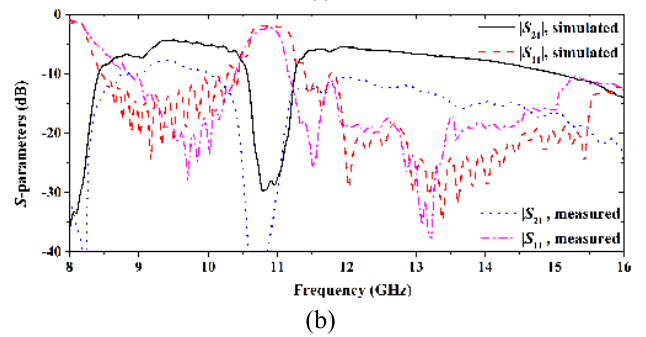
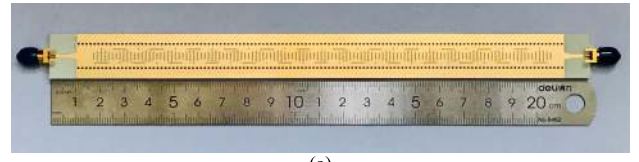


FIGURE 12. (a) Photo and (b) S-parameters of the proposed dual-beam and tri-band SIW LWA prototype.

of $\epsilon_r = 3.66$. The measured S-parameters of this prototype are depicted in Fig. 12 (b) in comparison with the simulated results. As can be seen, the simulated and measured $|S_{11}|$ are in good agreements with each other. However, the measured $|S_{21}|$ is lower than the simulated one, which means the SMA connectors and measurement errors cause additional losses during the experiment.

Fig. 13 demonstrates the simulated transient electric field distributions on the top wall ($z = 1.524$ mm) of two unit cells for the two periodic structures. It's clear that the first periodic structure produces vertical polarization wave (the electric field is parallel to the x -direction), and the second periodic structure produces horizontal polarization wave (the electric field is parallel to the y -direction). Therefore, the two beams of proposed antenna in band 3 are in different polarization directions, which means beam 1 generated by the

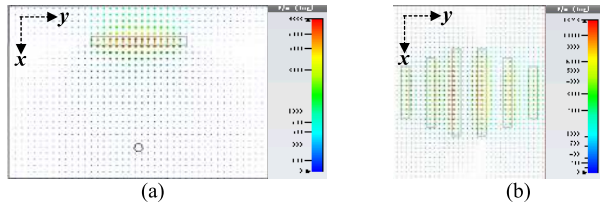


FIGURE 13. Transient electric field distributions on the top wall ($z = 1.524$ mm) of the two unit cells for: (a) first periodic structure, (b) second periodic structure.

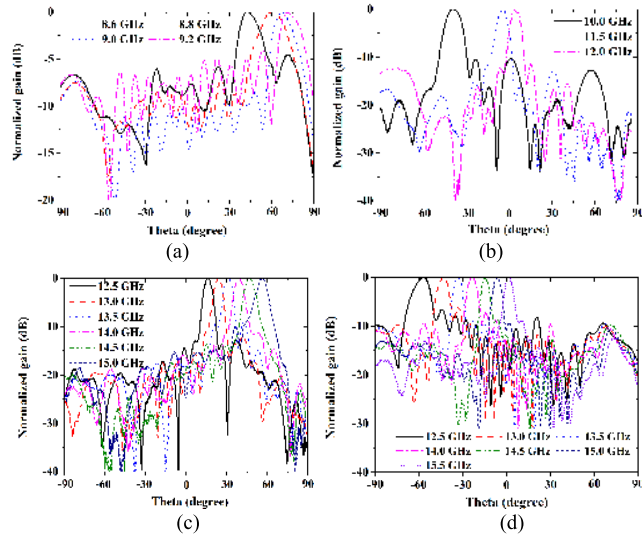


FIGURE 14. Measured radiation patterns (yoz-plane) of the proposed antennas in different frequency bands: (a) band 1, (b) band 2, (c) beam 1 in band 3, (d) beam 2 in band 3.

first periodic structure is in vertical polarization and beam 2 generated by the second periodic structure is in horizontal polarization. Similarly, the forward beam in band 1 generated by the second periodic structure is in horizontal polarization and the backward beam in band 2 generated by the first periodic structure is in vertical polarization.

In the measurement of radiation patterns, the proposed antenna is set to be the receiving antenna, and a standard linear polarized horn antenna working in the same frequency band is used as the transmitting antenna. So we need to separately measure the two different polarization beams in band 3 as shown in Fig. 14 (c) and (d). Fig. 14 (a) and (b) show the measured normalized gain patterns of the proposed antenna in band 1 and band 2, respectively. Compared with the simulated patterns, the beam angles of measured patterns are shifted a little and the side lobe level (SLL) is not as good as the simulated patterns, especially for the patterns plotted in Fig. 14 (a) and (d), which are generated by the second periodic structure. For the patterns generated by the first periodic structure as shown in Fig. 14 (b) and (c), due to the discrepancies between the measured stopband and the simulated stopband as observed from Fig. 12 (b), there are strong reflection beams and deteriorated gains in the patterns at 10.5 and 15.5 GHz, so they aren't given in the measured results.

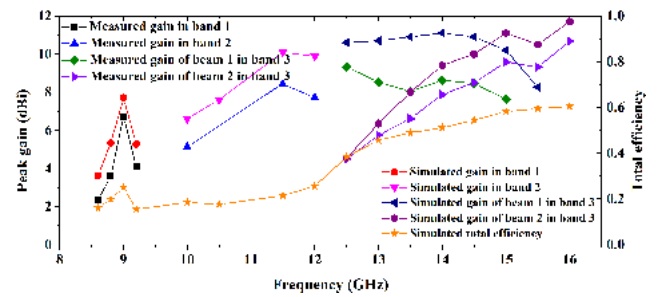


FIGURE 15. Measured and simulated gain and simulated total efficiency of the proposed antenna at different frequencies.

TABLE 2. Comparison between the proposed LWA and the similar artworks.

Ref.	Antenna type	Frequency (GHz)	Scanning range	Dual-beam	Broadside radiation
[24]	MSL	5.6~6.0	35°~42° -45°~34°	Yes	No
[25]	Dielectric	57~63	20°~30° -30°~20°	Yes	No
[33]	SIW	8.2~9.4 13.2~15.2	19°~78° 24°~84°	No	No
[34]	SIW	9.0~10.7 13.4~16.2	107°~167° -41°~114°	No	Yes
[37]	CRLH	57~62	-35°~34.5°	No	Yes
[38]	CRLH	55~65	-30°~30°	No	Yes
This work	SIW	8.6~9.2 10~12 12.5~15.5	42°~71° -40°~4° -55°~54°	Yes	Yes

The simulated and measured gain of the proposed antenna at different frequencies are summarized Fig. 15. As we can see, the measured gains are lower than the simulated ones due to the fabrication and measurement errors. As can be observed from Fig. 15, there are two broadside gain dips around 12 GHz and 15.5 GHz for beam 1 and beam 2, respectively, which are caused by the transversely symmetric antenna structure, so the Q balancing condition is not achieved and the consistent gain is not obtained [36]. Fig. 15 also gives the simulated results of total efficiency of the proposed antenna, which show the total efficiency is about 20% in band 1 and 2, and as the frequency increased to band 3, the efficiency of antenna increases to 60% or so. Table 2 summarizes the comparison between the proposed antenna and the similar available works, which shows the obvious advantages of this proposed LWA in the wide beam-scanning range including broadside direction, and the generation of dual-beam and tri-band radiation due to the novel structure.

IV. CONCLUSION

A novel dual-beam and tri-band SIW LWA with beam scanning including broadside direction is proposed and investigated. The dual-beam radiation is generated by two kinds of periodic structures working on -1st spatial harmonic modes which are combined in one antenna. The dispersion diagrams are analyzed to suppress the OSBs of both two periodic

structures, which makes the proposed antenna support the beam scanning in a wide angular range including broadside direction. Moreover, the second periodic structure has been optimized to realize the tri-band application. The results of measurement show that the proposed antenna has three operating frequency bands. In band 1 from 8.6 to 9.2 GHz, there is one beam scanning in forward region ($42^\circ \sim 71^\circ$), in band 2 from 10 to 12 GHz, there is one beam scanning in backward region ($-40^\circ \sim 4^\circ$), and in band 3 from 12.5 to 15.5 GHz, there is a dual-beam scanning from backward to forward including broadside ($-55^\circ \sim 54^\circ$).

REFERENCES

- [1] A. A. Oliner and D. R. Jackson, "Leaky-wave antennas," *Antenna Engineering Handbook*, J. Volakis, Ed., 4th ed. New York, NY, USA: McGraw-Hill, 2007, ch. 11.
- [2] M. Ettore, R. Sauleau, L. Le Coq, and F. Bodereau, "Single-folded leaky-wave antennas for automotive radars at 77 GHz," *IEEE Antennas Wireless Propag. Lett.*, vol. 9, pp. 859–862, 2010.
- [3] S. Gupta, S. Abielmona, and C. Caloz, "Microwave analog real-time spectrum analyzer (RTSA) based on the spectral-spatial decomposition property of leaky-wave structures," *IEEE Trans. Microw. Theory Techn.*, vol. 57, no. 12, pp. 2989–2999, Dec. 2009.
- [4] F. M. Monavar, S. Shamsinejad, R. Mirzavand, J. Melzer, and P. Mousavi, "Beam-steering SIW leaky-wave subarray with flat-topped footprint for 5G applications," *IEEE Trans. Antennas Propag.*, vol. 65, no. 3, pp. 1108–1120, Mar. 2017.
- [5] Y. J. Cheng, W. Hong, K. Wu, and Y. Fan, "Millimeter-wave substrate integrated waveguide long slot leaky-wave antennas and two-dimensional multibeam applications," *IEEE Trans. Antennas Propag.*, vol. 59, no. 1, pp. 40–47, Jan. 2011.
- [6] J. Liu, D. R. Jackson, and Y. Long, "Substrate integrated waveguide (SIW) leaky-wave antenna with transverse slots," *IEEE Trans. Antennas Propag.*, vol. 60, no. 1, pp. 20–29, Jan. 2012.
- [7] F. Xu, K. Wu, and X. Zhang, "Periodic leaky-wave antenna for millimeter wave applications based on substrate integrated waveguide," *IEEE Trans. Antennas Propag.*, vol. 58, no. 2, pp. 340–347, Feb. 2010.
- [8] J. Wang, Y. Geng, C. Zhang, and X. Huo, "Radiation characteristic of the periodic leaky wave structure and its application to leaky wave antenna design," in *Proc. Asia-Pacific Microw. Conf. (APMC)*, Nanjing, China, 2015, p. 1.
- [9] S. Paulotto, P. Baccarelli, F. Frezza, and D. R. Jackson, "A novel technique for open-stopband suppression in 1-D periodic printed leaky-wave antennas," *IEEE Trans. Antennas Propag.*, vol. 57, no. 7, pp. 1894–1906, Jul. 2009.
- [10] Y. L. Lyu, Xiao-Xin Liu, Peng-Yuan Wang, Daniel Erni, Qun Wu, Cong Wang, Nam-Young Kim, Fan-Yi Meng, "Leaky-wave antennas based on noncutoff substrate integrated waveguide supporting beam scanning from backward to forward," *IEEE Trans. Antennas Propag.*, vol. 64, no. 6, pp. 2155–2164, Jun. 2016.
- [11] J. Liu, W. Zhou, and Y. Long, "A simple technique for open-stopband suppression in periodic leaky-wave antennas using two nonidentical elements per unit cell," *IEEE Trans. Antennas Propag.*, vol. 66, no. 6, pp. 2741–2751, Jun. 2018.
- [12] R. Ranjan and J. Ghosh, "SIW-based leaky-wave antenna supporting wide range of beam scanning through broadside," *IEEE Antennas Wireless Propag. Lett.*, vol. 18, no. 4, pp. 606–610, Apr. 2019.
- [13] K. Solbach and B. Adelseck, "Dielectric image line leaky wave antenna for broadside radiation," *Electron. Lett.*, vol. 19, no. 16, pp. 640–641, Aug. 1983.
- [14] M. Guglielmi and D. R. Jackson, "Broadside radiation from periodic leaky-wave antennas," *IEEE Trans. Antennas Propag.*, vol. 41, no. 1, pp. 31–37, Jan. 1993.
- [15] S. Otto, A. Al-Bassam, A. Rennings, K. Solbach, and C. Caloz, "Transversal asymmetry in periodic leaky-wave antennas for Bloch impedance and radiation efficiency equalization through broadside," *IEEE Trans. Antennas Propag.*, vol. 62, no. 10, pp. 5037–5054, Oct. 2014.
- [16] A. Al-Bassam, S. Otto, D. Heberling, and C. Caloz, "Broadside dual-channel orthogonal-polarization radiation using a double-asymmetric periodic leaky-wave antenna," *IEEE Trans. Antennas Propag.*, vol. 65, no. 6, pp. 2855–2864, Jun. 2017.
- [17] M. Movahhedi, M. Karimipour, and N. Komjani, "Multibeam bidirectional wideband/wide-scanning-angle holographic leaky-wave antenna," *IEEE Antennas Wireless Propag. Lett.*, vol. 18, no. 7, pp. 1507–1511, Jul. 2019.
- [18] Y. Li, Q. Xue, E. K.-N. Yung, and Y. Long, "Dual-beam steering microstrip leaky wave antenna with fixed operating frequency," *IEEE Trans. Antennas Propag.*, vol. 56, no. 1, pp. 248–252, Jan. 2008.
- [19] A. Sarkar, S. Mukherjee, A. Sharma, A. Biswas, and M. J. Akhtar, "SIW-based quad-beam leaky-wave antenna with polarization diversity for four-quadrant scanning applications," *IEEE Trans. Antennas Propag.*, vol. 66, no. 8, pp. 3918–3925, Aug. 2018.
- [20] C.-C. Lin and C.-K. C. Tzuang, "A dual-beam micro-CPW leaky-mode antenna," *IEEE Trans. Antennas Propag.*, vol. 48, no. 2, pp. 310–316, Feb. 2000.
- [21] M. Garcia-Viguera, M. Esquius-Morote, J. Perruisseau-Carrier, and J. R. Mosig, "Dual-beam radiation from ID leaky-wave antennas," in *Proc. 8th Eur. Conf. Antennas Propag. (EuCAP)*, The Hague, The Netherlands, 2014, pp. 1447–1450.
- [22] C.-J. Wang, C. F. Jou, and J.-J. Wu, "A novel two-beam scanning active leaky-wave antenna," *IEEE Trans. Antennas Propag.*, vol. 47, no. 8, pp. 1314–1317, Aug. 1999.
- [23] C.-J. Wang, Y.-H. Sheu, and C. F. Jou, "A dual-beam asymmetrically scanning leaky-wave antenna by utilizing a HEMT resistive upconverter," *IEEE Microw. Wireless Compon. Lett.*, vol. 11, no. 12, pp. 492–494, Dec. 2001.
- [24] Z. L. Ma and L. J. Jiang, "One-dimensional triple periodic dual-beam microstrip leaky-wave antenna," *IEEE Antennas Wireless Propag. Lett.*, vol. 14, pp. 390–393, 2015.
- [25] Z. L. Ma, K. B. Ng, C. H. Chan, and L. J. Jiang, "A novel supercell-based dielectric grating dual-beam leaky-wave antenna for 60-GHz applications," *IEEE Trans. Antennas Propag.*, vol. 64, no. 12, pp. 5521–5526, Dec. 2016.
- [26] Y. Li and J. Wang, "Dual-band leaky-wave antenna based on dual-mode composite microstrip line for microwave and millimeter-wave applications," *IEEE Trans. Antennas Propag.*, vol. 66, no. 4, pp. 1660–1668, Apr. 2018.
- [27] G. V. Eleftheriades, "A generalized negative-refractive-index transmission-line (NRI-TL) metamaterial for dual-band and quad-band applications," *IEEE Microw. Compon. Lett.*, vol. 17, no. 6, pp. 415–417, Jun. 2007.
- [28] R. B. V. B. Simorangkir and Y. Lee, "A planar dual-band periodic leaky-wave antenna based on a mu-negative (MNG) transmission line," *IEEE Trans. Antennas Propag.*, vol. 63, no. 5, pp. 2370–2374, May 2015.
- [29] J. Machac, M. Polivka, and K. Zemlyakov, "A dual band leaky wave antenna on a CRLH substrate integrated waveguide," *IEEE Trans. Antennas Propag.*, vol. 61, no. 7, pp. 3876–3879, Jul. 2013.
- [30] S. S. Haghighi, A.-A. Heidari, and M. Movahhedi, "A three-band substrate integrated waveguide leaky-wave antenna based on composite right/left-handed structure," *IEEE Trans. Antennas Propag.*, vol. 63, no. 10, pp. 4578–4582, Oct. 2015.
- [31] D. K. Karmokar and K. P. Esselle, "Periodic U-slot-loaded dual-band half-width microstrip leaky-wave antennas for forward and backward beam scanning," *IEEE Trans. Antennas Propag.*, vol. 63, no. 12, pp. 5372–5381, Dec. 2015.
- [32] D. K. Karmokar, Y. J. Guo, P.-Y. Qin, K. P. Esselle, and T. S. Bird, "Forward and backward beam-scanning tri-band leaky-wave antenna," *IEEE Antennas Wireless Propag. Lett.*, vol. 16, pp. 1891–1894, 2017.
- [33] D. Wei, J. Li, J. Liu, G. Yang, and W. Zhang, "Dual-band substrate-integrated waveguide leaky-wave antenna with a simple feeding way," *IEEE Antennas Wireless Propag. Lett.*, vol. 18, no. 4, pp. 591–595, Apr. 2019.
- [34] Q. Zhang, Q. Zhang, H. Liu, and C. H. Chan, "Dual-band and dual-polarized leaky-wave antenna based on slotted SIW," *IEEE Antennas Wireless Propag. Lett.*, vol. 18, no. 3, pp. 507–511, Mar. 2019.
- [35] D.-F. Guan, Q. Zhang, P. You, Z.-B. Yang, Y. Zhou, and S.-W. Yong, "Scanning rate enhancement of leaky-wave antennas using slow-wave substrate integrated waveguide structure," *IEEE Trans. Antennas Propag.*, vol. 66, no. 7, pp. 3747–3751, Jul. 2018.
- [36] R. Shaw and M. K. Mandal, "Broadside scanning asymmetric SIW LWA with consistent gain and reduced sidelobe," *IEEE Trans. Antennas Propag.*, vol. 67, no. 2, pp. 823–833, Feb. 2019.

- [37] M. Alibakhshikenari, B. S. Virdee, M. Khalily, P. Shukla, C. H. See, R. A. Abd-Alhameed, F. Falcone, and E. Limiti, "Beam-scanning leaky-wave antenna based on CRLH-metamaterial for millimetre-wave applications," *IET Microw., Antennas Propag.*, vol. 13, no. 8, pp. 1129–1133, Jul. 2019.
- [38] M. Alibakhshikenari, B. S. Virdee, C. H. See, R. A. Abd-Alhameed, F. Falcone, and E. Limiti, "High-isolation leaky-wave array antenna based on CRLH-metamaterial implemented on SIW with $\pm 30^\circ$ frequency beam-scanning capability at millimetre-waves," *Electronics*, vol. 8, no. 6, p. 642, Jun. 2019.



YUNJIE GENG was born in Hebei, China. She received the B.Eng. degree in communications engineering from Beijing Jiaotong University, Beijing, China, in 2015, where she is currently pursuing the Ph.D. degree in electrical engineering.

From 2018 to 2019, she was a Visiting Student with the Poly-Grames Research Center, Polytechnique Montréal, University of Montreal, QC, Canada. Her current research interests include leaky-wave antennas and arrays. She has

served as a Reviewer for the IEEE ANTENNAS AND WIRELESS PROPAGATION LETTERS, IEEE ACCESS, and the *International Journal of Antennas and Propagation*.



JUNHONG WANG (M'02–SM'03) was born in Jiangsu, China, in 1965. He received the B.S. and M.S. degrees in electrical engineering from the University of Electronic Science and Technology of China, Chengdu, China, in 1988 and 1991, respectively, and the Ph.D. degree in electrical engineering from Southwest Jiaotong University, Chengdu, in 1994. In 1995, he joined Beijing Jiaotong University, Beijing, China, where he became a Professor, in 1999. From Jan-

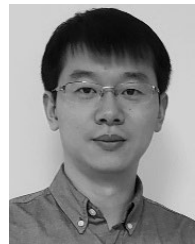
uary 1999 to June 2000, he was a Research Associate with the Department of Electric Engineering, City University of Hong Kong, Kowloon, Hong Kong. From July 2002 to July 2003, he was a Research Scientist with the Temasek Laboratories, National University of Singapore, Singapore. He is currently with the Key Laboratory of All Optical Network and Advanced Telecommunication Network, Ministry of Education of China, Beijing Jiaotong University, and the Institute of Lightwave Technology, Beijing Jiaotong University. His research interests include numerical methods, antennas, scattering, and leaky-wave structures.



ZHENG LI (M'15) received the B.S. degree in physics and the Ph.D. degree in electrical engineering from Beijing Jiaotong University, Beijing, China, in 2006 and 2012, respectively.

From 2008 to 2009, he was a Visiting Student with The Pennsylvania State University, PA, USA. From 2017 to 2018, he was a Visiting Professor with the Global Big Data Technologies Centre, University of Technology Sydney, Australia. In 2012, he joined the Faculty of the Department

of Electrical Engineering, Beijing Jiaotong University, where he became an Associate Professor, in 2015. His research interests include electrically beam scanning antennas and leaky-wave antennas.



YUJIAN LI (S'12–M'15) was born in Hunan, China, in 1987. He received the B.S. and M.S. degrees in communications engineering from Beijing Jiaotong University, Beijing, China, in 2009 and 2012, respectively, and the Ph.D. degree in electronic engineering from the City University of Hong Kong, in 2015.

In 2015, he joined the Institute of Lightwave Technology, Beijing Jiaotong University, where he is currently a Full Professor with the School

of Electronic and Information Engineering. His current research interests include millimeter wave antennas, base station antennas, and leaky-wave structures.

Dr. Li received the Outstanding Research Thesis Award from the City University of Hong Kong, in 2015, the Best Paper Award at the 2015 IEEE Asia-Pacific Conference on Antennas and Propagation (APCAP), the Best Student Paper at the 2013 National Conference on Antennas, and the Best Student Paper Award (Second Prize) at the 2013 IEEE International Workshop on Electromagnetics (iWEM). He was selected as a Finalist in the student paper contest of the 2015 IEEE AP-S Symposium on Antennas and Propagation (APS). He has served as a Reviewer for the IEEE TRANSACTIONS ON ANTENNAS AND PROPAGATION, the IEEE ANTENNAS AND WIRELESS PROPAGATION LETTERS, and the *IET Microwaves, Antennas and Propagation*.



MEIE CHEN received the B.S. degree in information and telecommunication engineering and the Ph.D. degree in electromagnetic and microwave technology from Beijing Jiaotong University, Beijing, China, in 2003 and 2009, respectively.

She is currently a Lecturer with the Institute of Lightwave Technology, Beijing Jiaotong University. Her research interests include antenna theory and technology, metasurface, and RCS reduction technique.



ZHAN ZHANG received the B.S. degree in electronics and communications engineering from Jilin University, China, in 2002, and the Ph.D. degree in electrical engineering from Nanyang Technological University, Singapore, in 2010. She joined the Faculty of the School of Electronics and Information Engineering, Beijing Jiaotong University, Beijing, China, in 2010, where she is currently an Associate Professor. Her current research interests include metamaterial-based antenna design and transformation optics.

...